COUPLING COMPLEX REFORMER CHEMICAL KINETICS WITH THREE-DIMENSIONAL COMPUTATIONAL FLUID DYNAMICS

Graham Goldin[a], Huayang Zhu[b], Kyle Kattke[b], Anthony M. Dean[b], Robert Braun[b], Robert J. Kee[b], Dan Zhang[c], Lubow Maier[c] and Olaf Deutchmann[c]

[a] ANSYS/Fluent, Lebanon, NH 03766, USA
[b] Engineering Division, Colorado School of Mines, Golden, CO 80401, USA
[c] University of Karlsruhe, Engesserstrasse 20, 76131 Karlsruhe, Germany

A new capability is developed that enables the modeling of certain logistics-fuel reformers. The system described in this paper considers a shell-and-tube configuration for which the catalytic reforming chemistry is confined within the tubes. The models are designed to accommodate detailed gas-phase and catalytic reaction kinetics, possibly including hundreds of species and thousands of reactions. The shell flow can be geometrically complex, but does not involve any complex chemistry. An iterative coupling algorithm is developed with which the geometrically complex flow is modeled with FLUENT and the chemically complex reforming is confined to straight tubes. The paper illustrates the model using propane partial oxidation and reforming as an example.

Introduction

Logistics-fuel reformers play essential roles in mobile SOFC applications such as auxiliary power units (APU). Modeling practical systems requires the coupling of geometric and fluid-mechanical complexity with chemical-kinetics complexity. The catalytic reforming kinetics of practical fuels (e.g., diesel fuel) depends upon gas-phase and heterogeneous reaction mechanisms that can involve over a thousand elementary reactions. Directly coupling chemistry at this level greatly exceeds the capability of computational fluid dynamics (CFD) models, which can handle geometric complexity.

The present paper describes a new capability to couple full chemical kinetics with computational fluid dynamics in FLUENT (www.ansys.com). The approach exploits the structure of reformers in which the combined gas-phase and catalytic chemistry is confined within geometrically simple tubes or channels. Flow over the external surfaces of the catalyst tubes is used to achieve thermal control. For example, hot exhaust products from an SOFC tail-gas combustor may be used to support endothermic steam reforming. Figure 1 illustrates such a configuration.

The coupling is accomplished with a User Defined Function (UDF) in FLUENT. Flow within the catalyst tubes is modeled with low-dimensional models that are written to accommodate chemical complexity using CHEMKIN, CANTERA, or DETCHEM interfaces. The outer fluid and thermal transport is modeled in FLUENT, which handles essentially arbitrary geometry. Coupling is via the exchange of temperature and heat-flux profiles at the tube walls. The UDF is written in C and provides the interface between geometrically complex three-dimensional outer mesh and the one-dimensional axial mesh for the catalyst tubes. In addition to outer fluid flow, the FLUENT model also represents solid-body heat transfer in the reactor walls and to the external environment.

The internal chemistry problem is solved using axial wall temperature profiles that are specified by FLUENT. Tube wall heat fluxes are predicted as a result of the chemically reacting flow problem within the tubes. These flux profiles are supplied to FLUENT via the UDF. FLUENT then solves the external problem using tube-wall heat fluxes as boundary conditions. The outer flow solution provides new tube-wall temperature profiles, which are used to solve the chemistry problem. The iterative process continues until convergence between the inner and outer problems. The capability is quite general in the sense that there are essentially no restrictions on the external flow of geometry or the chemistry and transport within the tubes.

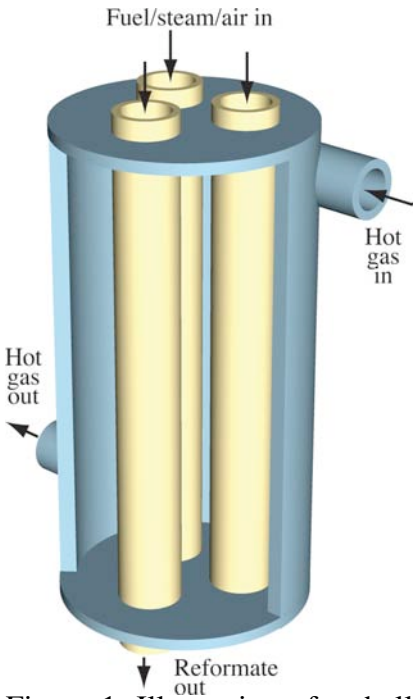

Figure 1: Illustration of a shell-and-tube reformer. Catalytic reforming proceeds within the tubes, with the outer shell flow used to assist control of the tube temperatures.

Coupling Algorithm

The coupling algorithm, implemented as a FLUENT UDF, must accomplish two primary functions. First, the algorithm must interpolate between three-dimensional meshes that are used by FLUENT and the one-dimensional band mesh used on the surface of the tubes. The second role of the UDF is to coordinate the iteration strategy between the outer CFD and the catalytic chemistry within the tubes.

In addition to the fluid flow regions, the CFD mesh resolves all the solid walls, including the tubes. The CFD mesh contains cylindrical "cut-outs" corresponding to the inner walls of the tubes. In other words, the inner tube walls are seen as boundaries for the CFD problem. The cylindrical CFD face mesh on the inside of each tube wall is sectioned into a user-specified number of bands as follows. The band spacing (one-dimensional mesh) is established to resolve gradients that characterize the interior catalytic chemistry problem. The UDF identifies the axis of the tube from its extents, and creates a unit axis vector in the direction of the interior tube flow. In the following discussion, "grid" refers to the one-dimensional band discretization and "mesh" refers to the collection of faces in the CFD discretization of the tube wall. An integer band number is identified as the linearly increasing cell index for the grid, with the first band in the first grid cell at the tube inlet. The UDF then loops over all mesh faces on a cylindrical tube and calculates the corresponding band number by projecting the face centroid onto the 1D grid.

Figure 2 illustrates the relationships between a general triangular surface mesh on a tube and the one-dimensional band grid. All triangular faces whose centroid touches the band are assigned to that band index. The band calculation is performed only once at the beginning of the simulation and the integer band number is stored for all mesh faces on the inner tube walls. As can be seen in Fig. 2 no special alignment is needed between the CFD mesh and the band grid.

At the beginning of each CFD iteration, the UDF calculates face-averaged temperatures for all bands in a tube. These band averages correspond to azimuthally averaged temperatures on the tube wall faces in the band. The UDF then writes out the list of the band temperatures to a file, and executes the 1D channel code. Typically, the

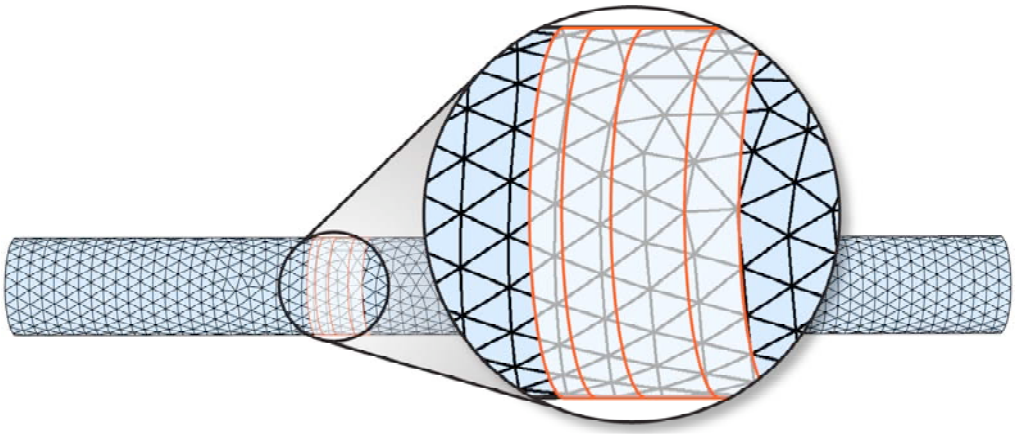

Figure 2: Illustration of three-dimensional FLUENT face mesh on a tube with an overlying one-dimensional band grid.

tube model is written to use the same discretization as the band grid. However, if the chemistry model uses a different spatial discretization then interpolation of the temperature from the band grid to the chemistry grid is required. When the tube simulation it complete, it writes a file containing the heat flux profile for the band grid. The UDF then reads these heat-flux profiles and assigns the fluxes in each band to the corresponding collection of mesh faces in that band. This procedure is repeated for all tubes. The CFD code solves the outer flow and heat transfer problem with the prescribed heat fluxes as boundary conditions. The iterative process of averaging tube temperatures in bands, solving the catalytic chemistry problem, transferring the heat fluxes back to the CFD model, and solving for the outer flow and temperature is repeated until convergence.

The UDF can perform a user-specified number of CFD flow and thermal iterations between tube-chemistry simulations. The inner tube-chemistry calculation is typically run to convergence for each intermediate tube-wall temperature profile as provided by the CFD model. In contrast, the CFD solution is always iterative, and hence, if the tube calculations are computationally expensive relative to the CFD calculations, overall convergence is accelerated by performing several CFD iterations between running the chemistry model.

It is possible that a reactor has a very large number of tubes and modeling detailed chemistry in all the tubes is impractical. Thus, the algorithm is generalized so that such groups of tubes can be modeled in terms of a few representative tubes. In other words, the wall temperatures of a cluster of tubes in the CFD mesh are averaged to one band grid. The chemistry problem is solved for the representative tube, with the resulting heat fluxes distributed back to all the tubes in the group.

Alternative Chemistry Models

The models are particularly concerned with complex catalytic reforming chemistry within the tubes. However, the specific geometric configuration within the tubes can vary considerably. Five types of internal configurations are commonly used:

- Plug flow within a tube having catalyst-coated walls
- Boundary-layer flow within a tube having catalyst-coated walls
- Tube filled with catalyst-coated ceramic foam
- Tube filled with a packed bed of catalyst particles
- Catalyst-coated multiple-channel monolith

Models for the chemically reacting flow within these different configurations are formulated and solved differently. Nevertheless, all can be coupled with the outer fluid-mechanically complex outer shell flow. The objective of the present paper is to discuss approaches and algorithms for coupling the fluid mechanically complex outer flow with the chemically complex flow within the tubes. The following paragraphs summarize some of the physical and computational aspects of different catalyst configurations within the tubes.

Chemically reacting plug flow

Plug flow provides the most straightforward representation of the catalytic reforming process. These models are formulated using the assumption that the gas flow within an open tube can be represented in terms of mean velocity, temperature, and chemical composition, all of which vary axially but not radially [1]. The model can be formulated either to include or exclude axial diffusive transport. Catalytic chemistry proceeds on the tube walls, and there may be homogeneous chemistry in the gas flow. Detailed catalytic reaction mechanisms usually involve gas-phase and surface-adsorbed species. Therefore, the conservation equations must include surface-species coverages. Heat and mass exchange between the gas and the catalytic surface can be represented in terms of heat- and mass-transfer coefficients, which can be evaluated from Reynolds-number correlations.

When axial diffusive transport is negligible, the plug-flow conservation equations form a system of differential-algebraic equations (DAE) [1, 2]. In this case, the computational solution begins with initial conditions (i.e., velocity, temperature, and composition) at the channel inlet and proceeds downstream to the channel exit. Software such as DASSL [3] or LIMEX [4] is specifically designed to solve these problems. When axial diffusion is retained, differential equations become a boundary-value problem, not an initial-value problem. Hybrid methods, such as implemented in TWOPNT [5] are effective in solving these problems [6].

Chemically reacting boundary-layer flow

Catalytically coated channels may be modeled using a boundary-layer formulation, which incorporates two-dimensional velocity, temperature, and composition fields within the gas phase [7]. By neglecting axial diffusive transport and assuming radially uniform pressure, the Navier-Stokes equations, which are elliptic partial differential equations, are converted to a parabolic system [1]. This formulation leads to a greatly more efficient computational solution [8–10]. Because the boundary-layer equations retain the two-dimensional axisymmetric nature of the gas flow, they provide an improved physical representation of the gas flow than the plug-flow equations do. Of course, this also comes at a relatively higher computational cost compared to plug flow.

Ceramic Foam Support

Coating a ceramic foam with a washcoat provides a good means to support the catalyst (Fig. 3). Compared to an open channel, such a structure provides significantly increased surface area as well as improved heat and mass transfer between the gas phase

and the catalyst. However, the pressure loss through the foam structure is higher than it is for an open channel.

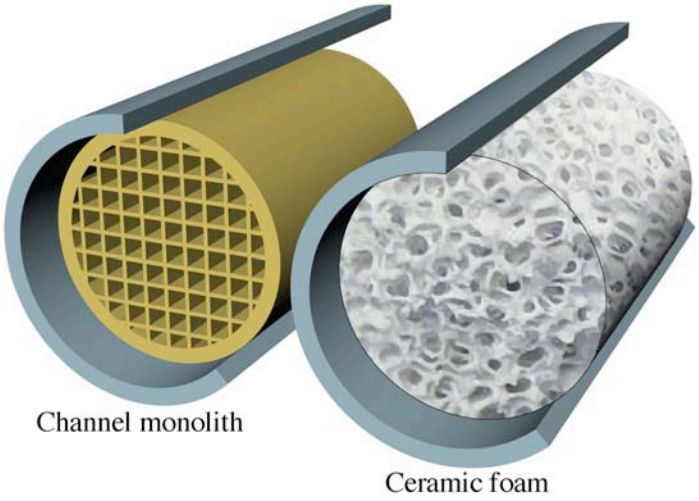

Figure 3: Catalysts inside the tubes may be supported on channel-monolith or ceramic-foam structures.

The diffusive and convective transport within the pore spaces of the foam can be modeled using the Dusty-Gas Model [11], which provides an implicit relationship between ordinary multicomponent diffusion, Knudsen diffusion, and Darcy flow. Incorporating the Dusty-Gas Model into mass-conservation equation that also includes the catalytic chemistry yields partial differential equations with elliptic spatial operators [12]. These equations may be solved computationally as a boundary-value problem (in steady state) or in differential-algebraic form to predict the transient response.

Packed Bed Catalyst

As an alternative to a porous-form support, the tube could be packed with catalyst pellets or powders. The mathematical problem is similar to that with porous foam, but the porous-media properties and catalyst surface areas may be very different.

Channel Monolith

Channel monoliths provide certain advantages for catalyst support. Catalysts washcoats are applied to the monolith walls. Compared to an open tube with catalysts on the tube wall, the monolith provides much more catalyst surface area. Compared to foam supports or packed beds, the channel monolith has significantly lower pressure losses.

Propane Reforming Chemistry

Modeling the reformation and partial oxidation of higher hydrocarbons requires understanding the complex interactions of gas-phase kinetics and heterogeneous surface chemistry. Because hydrocarbon fuels are sufficiently reactive that they begin to fragment or oxidize while still in the vapor phase, the species that interact with the catalyst surface are the reaction products of such chemistry. Species (including radicals) that desorb from the catalyst surface play important roles in the gas-phase kinetics, and hence the overall catalyst performance. The reaction mechanisms must represent a range of phenomena spanning from partial oxidation to pyrolysis [13, 14]. The gas-phase chemistry for the propane-reforming example discussed here consists of 511 elementary reaction steps among 54 gas-phase species.

The heterogeneous chemical reactions on the catalytic surface are modeled by a set of elementary-like reactions for the smaller hydrocarbons (C_{1-3}) and few additional lumped steps for adsorption of larger hydrocarbons (C_{2+}) assuming that their adsorption quickly

leads to the smaller molecules that are explicitly described by the detailed mechanism. The kinetics model is based on the mean field approximation (i.e., the catalytic surface is locally described by its mean coverage with adsorbed species and the temperature [1, 15]). The surface reaction rate is then expressed as function of coverage, temperature, and the gas phase concentrations close to the surface. The kinetic data for the elementary-like reactions are based on surface science studies including experimental data, theoretical studies using Density Functional Theory (DFT) and the semi-empirical Unity Bond Index-Quadratic Exponential Potential approach (UBI-QEP), and experimental evaluation by flow-reactor studies under technically relevant conditions. The mechanism is thermodynamically consistent, meaning that kinetic rates for forward and backward reactions are not independent and obey thermodynamic constraints. Estimation of kinetic data for lumped steps is based upon experimental information from flow-reactor studies.

The full surface-reaction mechanism consists of 104 reactions among 31 adsorbed and 26 gas-phase species. Homogeneous and heterogeneous chemistry is coupled not only by adsorption and desorption of stable reactants, intermediates, and products such as C_3H_8, C_3H_6, C_2H_6, C_2H_4, C_2H_2, CH_4, H_2, O_2, H_2O, CO_2, CO, but also of radical species such as H, O, OH, and many alkyls. In particular, understanding the interactions between homogeneous and heterogeneous reactions requires implementation of radical adsorption, which is a very efficient process (i.e., sticking probability close to unity). The most notable advantage of this rather complex approach for modeling catalytic chemistry is the fact that the mechanism includes all macroscopically relevant chemical processes such as partial and total oxidation, steam and CO_2 reforming, formation of olefins and other coke precursors, and formation of a carbonaceous over layer.

Illustrative Example

Consider propane reforming as an example to illustrate the coupled modeling capability. As illustrated in Fig. 4, three catalyst tubes are placed within the shell structure. The stainless-steel shell is 60 mm in diameter and 100 mm high. Hot air at 800 ˚C is supplied to and removed from the shell tangentially via rectangular slots (5 mm 10 mm). The mean inlet flow velocity ranges from 2.5 m/s to 10 m/s. Heat is removed from the outer shell walls to an ambient environment at 25 ˚C with a heat-transfer coefficient of 1 W/m^2K. The three-dimensional FLUENT simulation uses over 480,000 mesh cells to represent the turbulent shell flow.

The catalyst tubes for the present example are considered to be open tubes that are modeled using a plug-flow approximation. The stainless-steel tubes are 5 mm in diameter and 100 mm long, with a wall thickness of 1 mm. The inner walls are coated with a Rh-based catalyst that has an effective active area that is a factor of two greater than the geometric wall surface area.

The inlet fuel composition consists of 7.9% C_3H_8, 11.86% O_2, 44.64% N_2, and 35.60 % H_2O, which results in a carbon-to-oxygen ratio of unity and a steam-to-carbon ratio of 1.5. The mixture is supplied to the tubes at atmospheric pressure with an inlet velocity of 100 cm/s and an inlet temperature of 600 ˚C. Because of the relatively high O_2 content, the reaction of this mixture is net exothermic. That is, despite the H_2O content, the

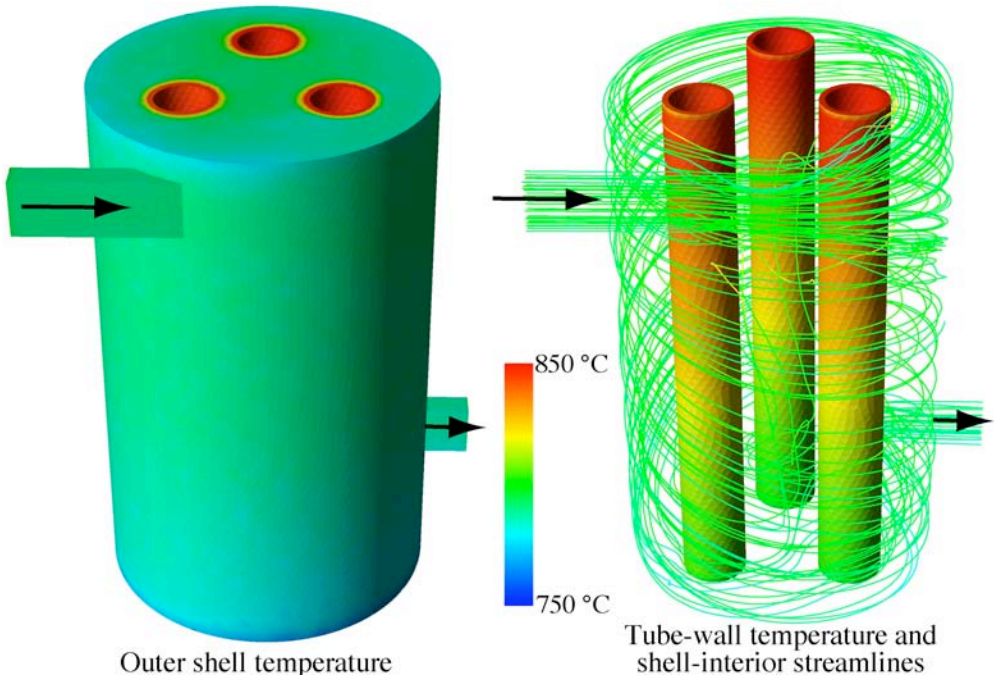

Figure 4: Shell wall temperature, tube wall temperature, and shell-interior air-flow streamlines. The vessel air inlet velocity is 10 m/s.

mixture behaves more like catalytic partial oxidation (CPOX) than it does like steam reforming.

Figure 4 illustrates some important features of the computational solution. The left-hand panel shows temperature of the outer shell skin. In this example, the outer shell temperature remains relatively close to the inlet temperature of 800 ˚C. The right-hand panel shows flow pathlines (colored by temperature) within the shell, superimposed on wall temperatures for the three reforming tubes. Because of the high circumferential inlet velocity, the highly circulating shell flow maintains very similar temperature profiles for each of the reforming tubes. Maintaining similar performance for all tubes is a desirable design objective.

The right-hand panel of Fig. 4 shows that the tube-wall temperatures are generally higher than the 800 ˚C shell gas, with tube inlet sections being nearly 50 ˚C higher than the shell gas. The tube temperature decreases along the length of the tube, which is the result of several factors. The entry region chemistry is dominated by relatively rapid partial exothermic partial oxidation. However, as

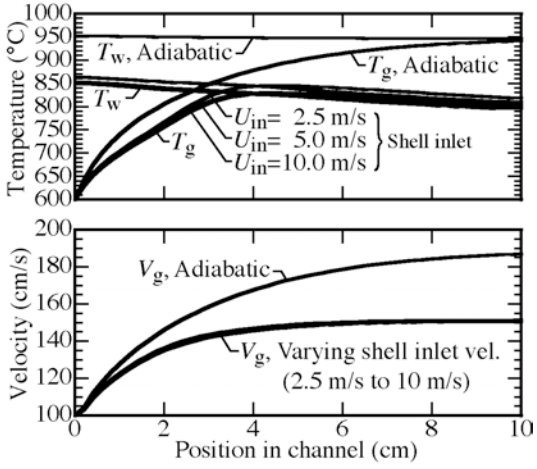

Figure 5: Comparison of the tube gas-phase temperature, tube wall temperature, and tube gas-phase velocity along the channel length for the vessel air inlet velocity of 2.5, 5, and 10 m/s. The plots also include the results of the adiabatic reacting tube flows.

the oxygen is depleted, endothermic steam reforming is more dominant in the downstream portions of the tube. Throughout the tube, heat transfer with the swirling shell gas tends to drive the tube temperature toward the shell-gas temperature.

Figure 5 shows profiles of gas-phase temperature and velocity within a tube for different shell-inlet velocities. As a point of reference, the figure also shows solutions that presume an adiabatic tube wall. Because of the exothermic partial oxidation, the temperatures for the adiabatic situation greatly exceed the temperatures for the shell-and-tube configuration. There is a relatively weak tube-temperature dependence for shell inlet velocities between 2.5 m/s and 10 m/s. However, as expected, higher shell flow increases heat-transfer and tends to lower tube temperatures. The gas velocity in the tube increases primarily because of increasing temperature and this lowering density.

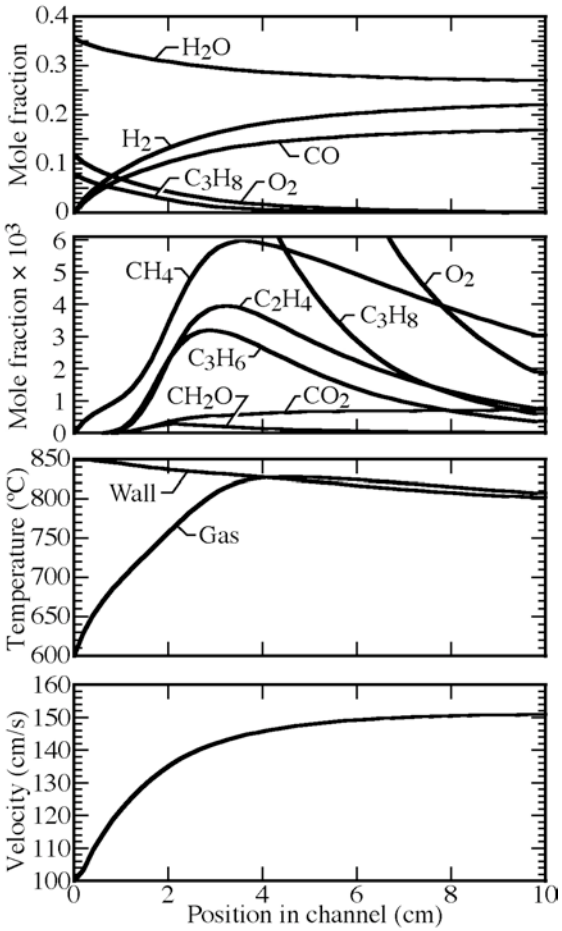

Figure 6: Profiles within a tube of gas-phase mole fractions for selected species, temperatures, and velocity. The shell inlet velocity is 10 m/s.

Figure 6 shows profiles within a tube of gas-phase mole fractions for selected species, temperatures, and velocity. The top panel shows major species, which follow expected reforming characteristics. That is, the C_3H_8, O_2 and H_2O all decrease, producing the desired syngas reformate mixture, H_2 and CO. The more interesting chemistry concerns the minor species. The small olefins (ethylene, C_2H_4, and propylene, C_3H_6) reach peak mole fractions of nearly 5×10^{-3}. These compounds are known to be problematic for certain downstream processes, such as a solid oxide fuel cell using a Ni-based anode. The present reactor reduces the olefin yield considerably before the reformate leaves the tubes. However, it is important to note that predictions such as these depend on the ability to couple complex chemistry with geometrically complex reactor design.

Summary and Conclusions

A new modeling capability has been developed, which, for certain reformer configurations, enables the coupling of complex catalytic chemistry and complex three-dimensional flow and heat transfer. Quantitative models for the reforming of hydrocarbon logistics fuels require large chemical reaction mechanisms that cannot be incorporated directly into any three-dimensional flow simulations. However, in configurations such as a shell-and-tube reactor the complex chemistry is confined within

fluid-mechanically simple tubes. The outer shell flow and heat transfer is fluid mechanically complex, but involves little or no chemistry. The approach described in this paper exploits this separation to develop practical computational models that assist reactor and process design.

Acknowledgments

This effort was supported in part by the Office of Naval Research via an RTC grant (N00014-05-1-03339).

References

1. R.J. Kee, M.E. Coltrin, and P. Glarborg, *Chemically Reacting Flow: Theory and Practice*, Wiley, Hoboken, NJ (2003).
2. U.M. Asher and L.R. Petzold, *Computer methods for ordinary differential equations and differential-algebraic equations*, SIAM, Philadelphia, PA (1998).
3. K. Brenan, S. Campbell, and L.R. Petzold, *Numerical solution of initial value problems in differential algebraic equations*, SIAM, Philadelphia, PA (1996).
4. P. Deuflhard, E. Hairer, and J. Zugck, *Num. Math.*, 51:501–516 (1987).
5. J.F. Grcar, *The TWOPNT program for boundary value problems*. Technical Report SAND91-8230, Sandia National Laboratories (1992).
6. J.F. Grcar, R.J. Kee, M.D. Smooke, and J.A. Miller, *Proc. Combust. Inst.*, 21:1773–1782 (1986).
7. L.L. Raja, R.J. Kee, O. Deutschmann, J. Warnatz, and L.D. Schmidt, *Catal. Today*, 59:47–60 (2000).
8. M.E. Coltrin, H.K. Moffat, R.J. Kee, and F.M. Rupley, *CRESLAF: A Fortran program for modeling laminar, chemically reacting, boundary-layer flow in cylindrical or planar channels*. Technical Report SAND93-0478, Sandia National Laboratories (1993).
9. S. Tischer, C. Correa, and O. Deutschmann, *Catal. Today*, 69:57–62 (2001).
10. H.D. Minh, H.G. Bock, S. Tischer, and O. Deutschmann, *AIChE J.*, 54:2432–2440 (2008).
11. E.A. Mason and A.P. Malinauskas. *Gas Transport in Porous Media: the Dusty-Gas Model,* American Elsevier, New York (1983).
12. H. Zhu, R.J. Kee, J.R. Engel, and D.T. Wickham, *Proc. Combust. Inst.*, 31:1965–1972 (2006).
13. K.L. Randolph and A.M. Dean, *Phys. Chem. Chem. Phys.*, 9:4245–4258 (2007).
14. C.V. Naik and A.M. Dean, *Proc. Combust. Inst.*, 32:437–443 (2007).
15. O. Deutschmann. Computational fluid dynamics simulation of catalytic reactors. In G. Ertl, H. Knözinger, F. Schüth, and J. Weitkamp, editors, Handbook of heterogeneous catalysis, Chapter 6.6. Wiley-VCH, 2nd edition, (2008).